

Structure of Electroless Nickel Coatings

By N.M. Martyak, S. Wetterer, L. Harrison, M. McNeil, R. Heu and A. Albert Neiderer

Electroless nickel (EN) coatings varying in occluded phosphorus were characterized using scanning tunneling (STM), electron microscopy (EM) and X-ray diffraction (XRD). Low-phosphorus (1 to 3 percent) EN coatings were crystalline and exhibited rounded mounds surrounded by fairly deep crevices. Medium- (4 to 7 percent) and high- (more than 9 percent) phosphorus deposits were generally amorphous and smooth. The effect of a small applied current on the structure was also determined.

Electroless nickel deposits (with phosphorus) are metastable phases in which phosphorus is occluded in a nickel matrix. The kinetics,¹⁻⁴ thermodynamics and mechanism⁵⁻⁷ of deposition have been well characterized. In addition, several of the unique properties, such as hardness,^{8,9} corrosion,^{10,11} and wear resistance,¹²⁻¹⁴ as well as magnetic properties^{14,15} offered by EN coatings have been investigated in detail. All of the properties of EN deposits are composition- and structure-dependent.

Low-phosphorus deposits (1 to 3 percent P) are crystalline and exhibit good wear resistance, but relatively poor corrosion resistance in a chloride environment. Medium-phosphorus deposits (5 to 8 percent P) have a smaller crystallite size and tend to be semi-amorphous, whereas high-phosphorus deposits (more than 10 percent P) exist mainly as a metallic glass. Medium-phosphorus deposits usually have properties lying between the low- or high-phosphorus deposits, but the solutions offer enhanced deposition rates. High-phosphorus deposits typically exhibit the best corrosion properties, but suffer from slow rates of deposition. In addition to the occluded phosphorus, the composition of the solution may affect deposit properties. Co-deposition of non-metallic stabilizers, similar to those used in electrolytic nickel solutions, may alter the surface appearance and, subsequently, the corrosion and wear resistance.

This study was undertaken to gain a better understanding of the effect of solution composition on the structure of electroless nickel coatings. In particular, deposits varying in percent phosphorus, as well as those deposited with a small applied current, were evaluated using scanning tunneling, transmission and scanning electron microscopy and X-ray diffraction.

Experimental Procedure

Each of the electroless nickel solutions contained 30 g/L NiSO₄, 30 g/L H₂PO₂, appropriate chelating, completing and buffering agents, along with metallic and non-metallic stabilizers. The pH of the low-, medium- and high-phosphorus solutions was 6.8, 4.8 and 4.7, respectively. All solutions were operated at 90 °C.

The preplating treatment of the steel substrates was a soak in a strong alkaline cleaner at 80 °C for three rein, followed by a cold-water rinse. The parts were then anodically cleaned at 6.0 V, for 30 see, at 75 °C in 50 g/L NaOH, again followed by a cold-water rinse. After immersion in 5-percent HCl, for 3 see, at room temperature and a cold-water rinse, the parts were plated with electroless nickel.

Similarly, copper foil was cut to approximately 5 x 5 cm and masked with stop-off material, exposing a square of about 25 cm². The copper was electropolished in 67-percent H₃PO₄ at 1.7 V for 3 min. The sample was rinsed in 10-percent H₂PO₄, followed by two water rinses. The sample was placed in the EN solution and allowed to warm up for 5 min. It was necessary to initiate EN deposition by placing the copper foil in contact with a piece of iron.

The surface structures of the electroless nickel deposits were examined by scanning tunneling microscopy, STM^a. Sections of the electroless nickel films attached to their steel or copper substrates were cut and placed on the stage of the STM cell. Two different scanning heads, 1.0 μm and 12 μm, were used, as were various scanning speeds. Platinum-iridium tips were used for atomic-scale imaging, whereas tungsten was used for imaging of irregular surfaces.

The surface of the electroless nickel films was also examined using scanning electron microscopy.^b Samples were mounted using carbon or silver paste to ground them. Chemical analyses were performed by energy dispersive spectroscopy (EDS). Dot mapping for phosphorus and nickel was also performed on several samples.

The structures of thin EN films of various as-deposited thicknesses were studied using transmission electron microscopy (TEM).^c Electroless nickel films 20 to 100 nm thick were deposited on the copper substrates. The substrates were masked using stop-off material so as to expose a 3-cm² area. After plating, the masking material was removed in acetone. The copper substrates were then dissolved by floating the sample on a solution containing 500 g/L CrO₃ and 50 mL/L H₂SO₄ at room temperature. The electroless nickel foil was then rinsed several times in distilled water, mounted on copper grids

^a Digital Instruments, Inc., Santa Barbara, CA

^b Cambridge MK3 Steroscan, Cambridge, MD

^c Philips 430 Transmission Electron Microscope, Eindhoven, Netherlands

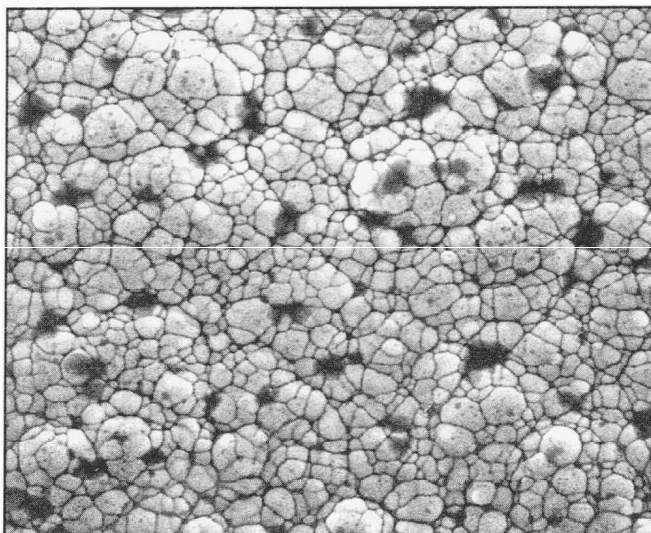


Fig. 1—SEM of low-phosphorus EN coating.

Lattice Parameters

Deposit	Calculated (Å)
Low-P	3.5031
Low-P (w/current)	3.5034
Medium-P	3.4771
Medium-P (w/current)	3.4934
High-P	3.6034
High-P (w/current)	—

and dried with methanol. EDS was performed for phosphorus, sulfur and nickel.

X-ray diffraction (XRD)⁴ patterns were recorded for electroless nickel deposits with thicknesses in the range of 25 μm. A step scan with a long count time was used while recording the diffraction patterns. Instrument settings were:

Radiation: Cu-K_α, 1.5406 nm
 Automatic Divergent Slit
 Tube Current: 35 mA at 45 kV
 Step Size: 0.02°
 Sample Time: 4.0 sec
 Peak Angle Range: 5-100°

Results

A scanning electron micrograph of low-phosphorus EN, shown in Fig. 1, exhibits a rounded-mound structure surrounded by fairly deep crevices. The size of the nodules varies from 0.1 to 1 μm. An STM micrograph of the same sample, Fig. 2, is similar to the SEM image; the lateral dimension of the nodules is approximately 0.2 μm. STM also revealed that the depth of the crevices is 0.01 to 0.02 μm. Medium-phosphorus EN deposits exhibited a more uniform surface structure, too fine, however, to resolve with SEM. Small surface crevices on the order of 3 to 8 nm were seen, using the STM. Small surface protrusions were also observed in the medium-phosphorus coatings. Atomic-scale features of the medium-phosphorus EN deposit are shown in Fig. 3, an STM line plot. High-phosphorus EN deposits were even smoother than the medium-phosphorus EN deposits. An STM surface image is shown in Fig. 4.

An applied current increased the size of the surface nodules in the low-phosphorus EN deposits. The medium- and high-phosphorus deposits also developed a very nodular surface. The sizes of the nodules were approximately 0.5 to 2 μm across and 0.02 to 0.05 μm deep.

⁴ Philips Automated Powder Diffractometer APD 3720, Eindhoven, Netherlands

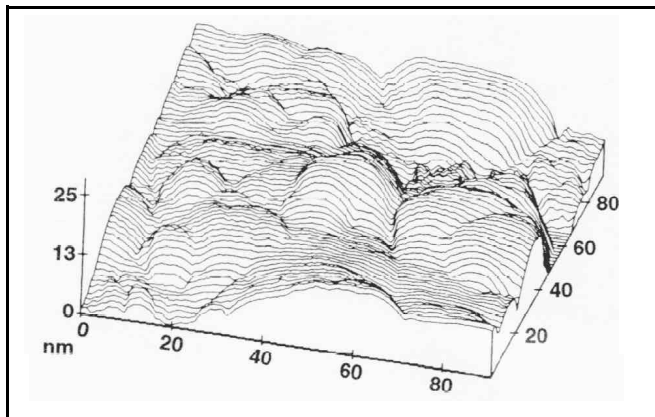


Fig. 2—STM of low-phosphorus EN deposit.

Transmission electron micrographs of EN deposits plated in the low-, medium- and high-phosphorus solutions, Figs. 5, 6 and 7, show a clear distinction in the initial growth mode. Low-phosphorus EN deposits began as discrete islands that grew into a continuous film. Growth of these islands appears to be isotropic. Nucleation started at specific sites on the substrate and, with continued growth, coalesced into a continuous film. The size of the individual islands is very close in size to the nodules observed in the STM and SEM images. TEM-EDS of the crevice region, Fig. 5, reveals a significant amount of occluded sulfur. Electron diffraction confirmed the crystallinity of these deposits. Medium-phosphorus deposits were more continuous with fewer island-like structures. Amorphous rings with diffraction spots superimposed on these rings indicate a semi-amorphous structure. High-phosphorus deposits grew more uniformly and appeared to spread as layers with no signs of island growth. Diffraction patterns confirmed the amorphous structure of these deposits.

X-ray diffraction studies showed that low-phosphorus EN deposits in the as-plated condition (without an applied current) were crystalline and exhibited a strong (111) preferred orientation (Fig. 8). An asymmetric tail on the low d-spacing side of the (111) was observed. Low-phosphorus coatings deposited with an applied current were amorphous. The XRD pattern of the medium-phosphorus deposits, with and without current, also exhibited amorphous structures. In both deposits, there was an overlap between the (111) and (200) orientations (Fig. 9). The high-phosphorus deposits were very similar to the medium-phosphorus deposits—amorphous, but with an asymmetric (111) tail.

The calculated lattice parameter for nickel was determined from the maximum intensity of the (111) reflection:

$$1/d^2 = (h^2 + k^2 + l^2)/a^2$$

The lattice parameters were as given in the table.

Discussion

The three structures observed in this study are dependent upon the composition of the plating solution and deposition parameters. Thin films of low-phosphorus electroless nickel were crystalline and discontinuous. As the percent occluded phosphorus in the coatings increased, the structure changed to a more continuous structure with a concomitant decrease in crystallinity. Previously, various growth modes of electroless nickel on different surfaces have been observed.^{16,17} The initial structure of EN deposits has been associated with different modes of activation of the substrate. Copper is not catalytically

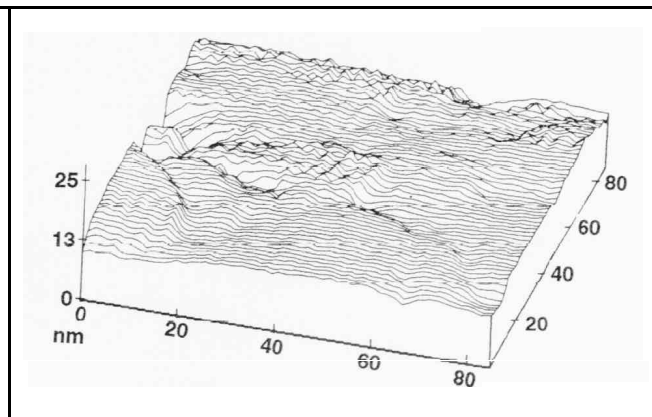


Fig. 3—STM of medium-phosphorus EN deposit.

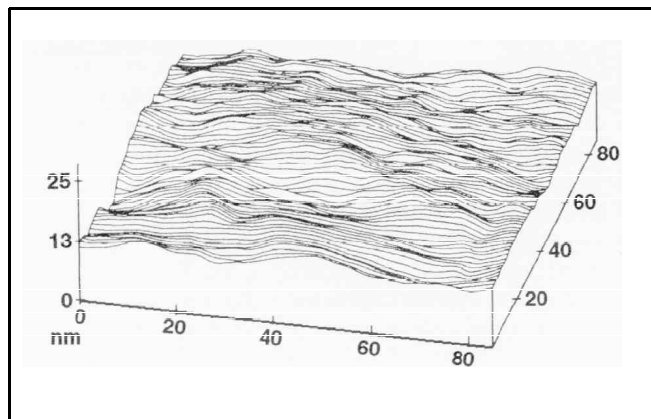


Fig. 4—STM of high-phosphorus EN deposit.

active with respect to oxidation of H_2PO_2 ;¹⁸ there is normally an induction period prior to the deposition of nickel. In addition, copper is a noble metal, reacting with oxygen and water more readily than Hg or Ag. This tendency to form surface oxide films, both Cu_2O and CuO , is pH-dependent and would thus change the number of activation sites, thereby altering the structure of the initial EN deposits. The pH of the low-phosphorus EN solution is considerably higher than that of the medium- or high-phosphorus. The potential-pH coordinates (-0.295 V vs. SCE, pH 6.8) of a copper electrode in the low-phosphorus solution is in the Cu_2O domain of stability; however, at pH 4.7 and 4.8, metallic copper is the most thermodynamically stable species.¹⁹ Accordingly, the surface of the copper electrode is different in the three solutions. Marton and Schlesinger have shown that the critical film thickness at which the EN deposit is continuous is dependent upon the density of active surface sites for nucleation.¹⁶ Similarly, Cortijo and Schlesinger showed that EN structures were dependent upon the pH of the solution. "

The initial structure observed in the TEM images appeared to continue into the bulk. Deposits from low-phosphorus solutions were dull, whereas the medium- and high-phosphorus deposits were bright. The dull appearance of the low-phosphorus deposits is a result of the surface structure. The relationship between brightness and the structure of the electrodeposits has been studied. Weil and Paquin showed that the percentage of reflected light decreased with surface roughness.²⁰ The surface roughness and, consequently, brightness are depen-

dent upon the degree to which the surface structure is in one plane and are influenced by the percentage of included foreign substances and grain sizes. The boundaries of large grains are usually deep grooves. It is therefore a necessary condition that bright deposits be fine-grained. A fine-grained deposit does not ensure, however, that the coating will be bright. Small additions of thiourea to Watts nickel solutions, for example, formed groups of fine-grained material surrounded by crevices. With increasing thickness, the crevices became deeper, with a resulting loss in brightness.

Previously, the formation of crevices was shown to depend on the distribution of occluded addition agents. There is considerable evidence that in nickel deposits, if a control agent is concentrated in some surface locations, growth is impeded there and crevices develop.²⁰⁻²² Rogers et al.²³ confirmed the results of Beacom and Riley,²² showing preferential adsorption of sulfur ions on the high-current-density areas of the deposit. Once adsorbed, growth is impeded and crevices formed. TEM-EDS analysis showed that the percentage of occluded sulfur was greater in the grooves of the low-phosphorus deposits than at the top of the rounded-mound structure. It is likely that this non-random distribution of sulfur, from thiourea additions, impeded growth and resulted in the crevice-like structure, similar to that observed in electrolytic nickel deposits.

All deposits plated with the applied current were dull and had a very rough surface structure. Hoekstra and Trivich showed that control agents in electrolytic nickel solutions do not decompose in the presence of nickel, but occluded sulfur in nickel is found only after electrolysis." The applied current may have assisted thiourea decomposition, causing a greater non-random-distribution of sulfur, similar to that discussed above.

The scanning electron micrographs and scanning tunneling images are very similar, showing the lateral size of the rounded-mound structure. However, STM has also revealed that the depth of the crevices is on the order of 0.02 μm . The structure and dimensions of this configuration have much significance in terms of corrosion protection.

The texture observed in low-phosphorus coatings indicates that some crystallographic planes did not develop. It has been postulated that the development of a texture in electrodeposited metals is a result of supersaturation (i.e., overvoltage) used to deposit the metal^{25,26} or the adsorption of foreign materials;²⁷ however, there was no mention of texturing in electroless metal deposits. Graham et al. have discussed possible preferential

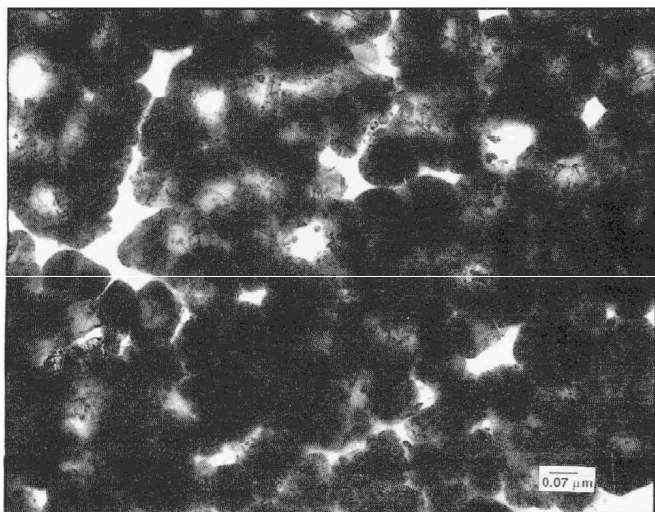


Fig. 5—TEM of low-phosphorus EN coating.

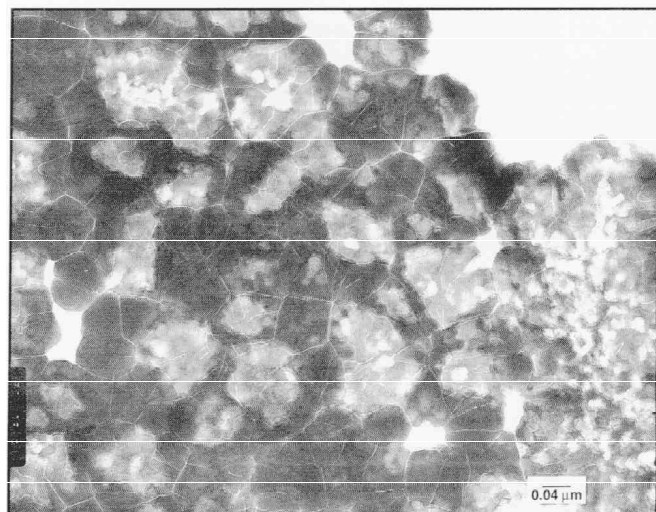


Fig. 6—TEM of medium-phosphorus EN coating.



Fig. 7—TEM of high-phosphorus EN coating.

adsorption of phosphorus on certain planes.²⁸ If adsorbed, these planes would be retarded from growing, with the resultant structure possessing a preferred orientation. Medium- and high-phosphorus coatings appeared to be more amorphous, even though the electron diffraction patterns showed some evidence of crystallinity. Factors which broadened x-ray diffraction patterns include a small crystallite size, elastic strains and stacking faults. It is likely that the smaller sizes of the diffracting domains is responsible for the broad patterns. Goldenstein *et al.*²⁹ and Graham *et al.*²⁸ have calculated the crystallite size from x-ray line broadening and have shown a decrease in particle size with an increase in the phosphorus content. It is also possible that a preferred orientation exists in the medium- and high-phosphorus deposits. A strong texture exists in electrodeposited chromium samples³⁰ and only a broad (222) reflection is observed. The fact that only one reflection in chromium deposits is observed does not indicate an amorphous structure but rather a textured deposit coupled with a small crystallite size. Similarly, if a [111] fiber texture exists in the medium- and high-phosphorus deposits, coupled with a small crystallite size, the predominant reflection would be the (111) and it would be severely broadened. The asymmetry associated with the (111) also implies that stacking faults made some contribution to the broadening.

The patterns from the low-phosphorus alloys clearly show the effect of stacking faults on the {111} and {200} reflections. Paterson also demonstrated the effect of stacking faults in fcc metals on the resultant diffraction profile.³¹ Stacking faults shift all the {111} except the (111) and (111) reflections to lower *d* spacings (higher reciprocal *d*-spacings) and tend to broaden the reflections. Similarly, the presence of stacking faults decreases the intensity of the {200} reflections and shifts all six to high *d*-spacings. As a result, the high-angle side of the {111} and the low-angle side of the {200} reflections overlap.

The calculated lattice parameter of nickel in electroless nickel is slightly different from that of elemental nickel, 3.5238 Å, which may result from the occluded phosphorus. The atomic radius of nickel, 1.28 Å, is about 3 percent greater than that of phosphorus, 1.24 Å. This difference, coupled with the large amount of occluded phosphorus, maybe enough to account for the approximate 0.2 to 0.7 percent difference in lattice parameters. It has been shown that small additions of phosphorus, 0.58 w/w percent, to copper alters the lattice parameter of copper even though the atomic radii of copper and phosphorus are identical.³²

Conclusions

The structures of EN coatings varying in occluded phosphorus were characterized using STM, TEM, SEM and XRD. The initial structures of low-phosphorus deposits were island-like whereas medium- and high-phosphorus deposits were more continuous. The initial structure appears to be dependent upon the solution composition and PH. STM results showed that the structure in thin films continues into the bulk, with low-phosphorus coatings possessing a rough surface structure. The crevices are the result of a non-random distribution of occluded sulfur. Deposits with less than 7 percent phosphorus are highly oriented, whereas medium-phosphorus deposits are semi-amorphous. XRD and electron diffraction revealed that high-phosphorus deposits are amorphous.

References

1. J. Flis and D.J. Duquette, *J. Electrochem. Soc.*, 131, 34 (1984).
2. G.O. Mallory and V.A. Lloyd, *Plat. and Surf. Fin.*, 72, 52 (Sept., 1985).
3. G. Gutzeit, *Plating*, 47,63 (Jan., 1960).
4. R.M. Lukes, *Plating*, 51, 969(1964).

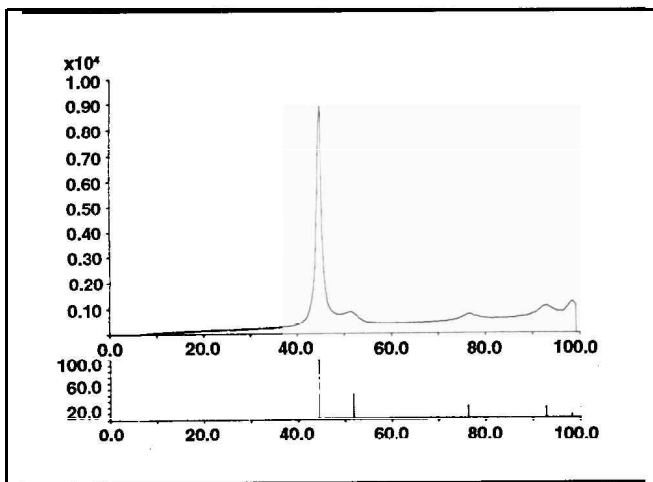


Fig. 8-XRD pattern of low-phosphorus coating.

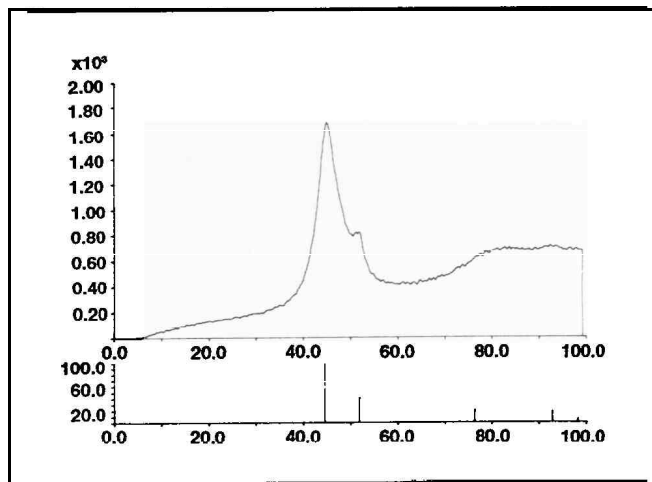
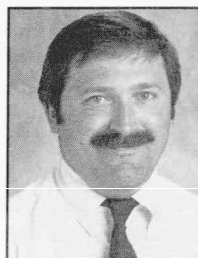


Fig. 9-XRD pattern of medium-phosphorus coating (with current).

5. J.P. Randin and H.E. Hintermann, *J. Electrochem. Soc.*, 117, 160 (1970).
6. N.M. Martyak, Unpublished results (1 991).
7. N. Feldstein and T.S. Lancsek, *J. Electrochem. Soc.*, 118, 869 (1971).
8. S.H. Park and D.N. Lee, *J. Materials Science*, 23, 1643 (1988).
9. Q.X. Mai, R.D. Daniels and H.B. Harpalani, *Thin Solid Films*, 166, 235(1988).
10. S.S. Tuli, *Trans. IMF*, 64,73 (1986).
11. M. Sadeghi, P.D. Longfield and C.F. Beer, *Trans. IMF*, 61, 141 (1983).
12. U. Ma and D.T. Gawne, *Trans. IMF* 63,64(1985).
13. K.M. Gorbunova, M.V. Ivanov and V.P. Moiseev, *J. Electrochem. Soc.*, 120, 613 (1973).
14. G.G. Gawrilov, *Chemical (Electroless) Plating*, Portcullis Press, Redhill, Surrey, UK (1979).
15. A. Brenner, D. Couch and E. Williams, *J. Res. Nat Bureau Stds.*, 44, (1950).
16. J.P. Marton and M. Schlesinger, *J. Electrochem. Soc.*, 115, 16 (1968).
17. R.O. Cortijo and M. Schlesinger, *ibid.*, 130,2341 (1983).
18. I. Ohno, O. Wakabayashi and S. Haruyama, *ibid.*, 132, 2323 (1 985).
19. N.M. Martyak, Submitted to *J. Electrochem. Soc.* (1993).
20. R. Weil and J. Paquin, *J. Electrochem. Soc.*, 107, 87 (1960).
21. R. Weil and H.C. Cook, *ibid.*, 109,295 (1962).
22. S.E. Beacom and B.J. Riley, *ibid.*, 108, 758(1961).
23. G.T. Rogers, M.J. Ware and R.V. Fellows, *ibid.*, 107,677 (1960).
24. J.J. Hoekstra and D. Trivich, *ibid.*,111, 162 (1964).
25. S. Rashkov, D.S. Stoichev and I. Tomov, *Electrochim. Acts*, 17, 1955 (1972).
26. N.A. Pangarov, *ibid.*, 9, 721 (1964).
27. A.K.N. Reddy, *J. Electroanal. Chem.*, 6, 141 (1963).
28. A.H. Graham, R.W. Lindsay and H.J. Read, *J. Electrochem. Soc.*, 112,401 (1965).
29. A.W. Goldenstein, W. Rostoker, F. Schossberger and G. Gutzeit, *ibid.*, 104, 104(1957).
30. N.M. Martyak, PhD Dissertation, Stevens Institute of Technology, Hoboken, NJ (1991).
31. M.S. Paterson, *J. Appl. Phys.*, 23, 805(1952).
32. W.B. Pearson, *A Handbook of Lattice Spacings and Structure of Metals and Alloys*, Pergamon Press, New York, NY, 1958.



Martyak

About the Authors

Dr. Nicholas M. Martyak, CEF, is a senior research chemist in the Advanced Performance Materials Group of Monsanto Chemical Co., APM, Q1E, 800 N. Lindbergh Blvd., St. Louis, MO 63167. He holds an MS in chemistry from the State University of New York, Binghamton, and a PhD in materials science and engineering from Stevens Institute of Technology, Hoboken, NJ. He has been awarded several U.S. patents and has others pending.

Sean Wetterer is a graduate of the California Institute of Technology with a dual major in chemistry and materials science. His research interests include the structure-property relationships of electrodeposited materials, corrosion, and computer modeling of electrochemical processes. He has published several papers in these fields and will attend graduate school for an advanced degree in chemistry.

L.D. Harrison is research manager for Atotech USA, specializing in functional coating development. He holds a BS in chemistry from Wayne State University and has more than 33 years' experience in metal finishing. His research interests include electroless nickel, composite plating, and corrosion-resistant coatings.

Dr. M.W. McNeil is a senior research chemist for Atotech USA. He holds a BS in chemistry from the University of Virginia and a PhD in organic chemistry from Penn State University. His assignments include electroless nickel product development and application research.

R.T. Heu is a researcher in the Microscopy Laboratory of Colgate-Palmolive Co., Piscataway, NJ. He holds a B. Eng. and MS in metallurgy from Stevens Institute of Technology. He is working in the field of materials characterization, concentrating on SEM, EDX analysis, XRD analysis and scanning probe microscopy.

A.A. Neiderer, CEF, is a chemist in the R&D Division of Atotech USA. He holds a BS in chemistry from the University of Pennsylvania-Shippensburg. His research interests include corrosion of chromium electrodeposits, EN/Cr duplex coatings and microcracking of thick chromium electrodeposits, as well as metallography and tribology of electrodeposited coatings.